

A SPECTRAL METHOD WITH STAGGERED GRID FOR INCOMPRESSIBLE NAVIER–STOKES EQUATIONS

F. MONTIGNY-RANNOU AND Y. MORCHOISNE

Office National d'Etudes et de Recherches Aéropatiales, BP 72-92322 Châtillon Cedex, France

SUMMARY

In order to solve the Navier–Stokes equations by spectral methods, we develop an algorithm using a staggered grid to compute the pressure. On this grid, an iterative process based on an artificial compressibility matrix associates the pressure with the continuity equation. This method is very accurate and avoids naturally most of the effects of parasite modes appearing in classical spectral methods with a velocity–pressure formulation.

KEY WORDS Incompressible Navier–Stokes Equations Spectral Method Artificial Compressibility Square Cavity

INTRODUCTION

When solving the incompressible Navier–Stokes equations for an inhomogeneous flow, difficulties arise during pressure computation. There are two classical ways of solving these problems.

The first one consists of taking the divergence of the momentum equation and using the continuity equation; we obtain a Poisson equation for the pressure. The unknowns are coupled by boundary conditions for the pressure (normal component of the momentum equation). Some compatibility conditions have to be satisfied to avoid singularities at the first time step.^{1,2}

The second one consists of solving simultaneously the momentum equation and the continuity equation.^{3,4} We have made some tests, and the results obtained on the Stokes problem are better with the second technique.³

Morchoisne^{5,6} has built a technique with an operator joining up the pressure with the velocity divergence on the same grid. This method can be compared with the influence matrix method.⁷ Some parasite modes for the pressure are found and have to be ‘filtered’ whichever numerical method is used.⁸

The purpose of the present paper is to solve the two-dimensional Navier–Stokes equations with a staggered grid; we use an iterative process with an approximation of the operator connecting pressure to velocity divergence. With the staggered grid, seven of the eight parasite modes seem to be naturally eliminated (the constant mode remains).

The studied problem is presented; then the method is developed and an application to the regularized square cavity problem is given.

PROBLEM STATEMENT

Consider the two-dimensional Navier–Stokes problem defined in a square domain Ω for a viscous incompressible fluid. The equations are

Momentum equation

$$\frac{\partial \mathbf{U}}{\partial t} = -\nabla P - (\mathbf{U} \cdot \nabla) \mathbf{U} + \nu \Delta \mathbf{U}, \quad \forall t \in [0, T], \quad \forall \mathbf{x} \in \Omega =]-1, +1[^2. \quad (1)$$

Continuity equation

$$\nabla \cdot \mathbf{U} = 0, \quad \forall t \in [0, T], \quad \forall \mathbf{x} \in \Omega =]-1, +1[^2. \quad (2)$$

Boundary conditions

$$\mathbf{U} = \mathbf{U}_B, \quad \forall \mathbf{x} \in \partial\Omega, \quad \forall t \in [0, T]. \quad (3)$$

Initial conditions satisfying boundary conditions (3)

$$\mathbf{U} = \mathbf{U}_0, \quad t = 0 \quad \forall \mathbf{x} \in \Omega. \quad (4)$$

The velocity \mathbf{U} is defined at the classical Chebyshev grid points (\times on Figure 1). Their coordinates are

$$x_i = \cos\left(\frac{\pi(i-1)}{N_x-1}\right), \quad y_j = \cos\left(\frac{\pi(j-1)}{N_y-1}\right), \quad (5)$$

where N_x and N_y are the number of discretization points in the x and y directions, respectively. The momentum equation (1) is solved on that grid with boundary conditions (3).

The pressure P is defined at the staggered Chebyshev grid points (\bullet on Figure 1). Their coordinates are

$$x'_i = \cos\left(\frac{\pi(2i-1)}{2(N_x-1)}\right), \quad y'_j = \cos\left(\frac{\pi(2j-1)}{2(N_y-1)}\right). \quad (6)$$

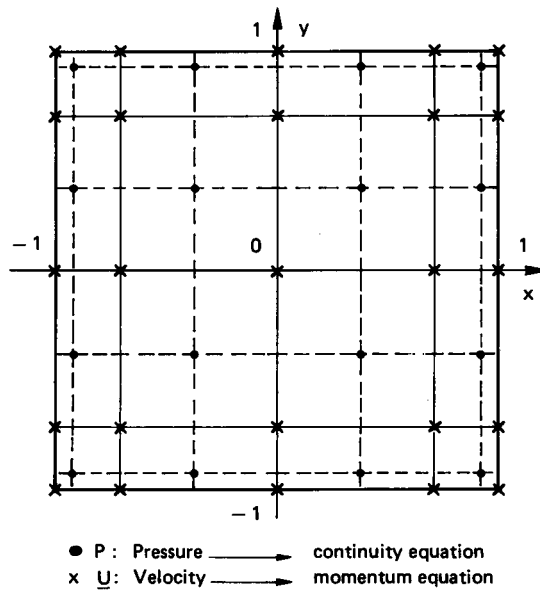


Figure 1. Staggered grid with Chebyshev collocation points (example: $N_x = N_y = 5$)

The continuity equation (2) is solved on the grid with $(N_x - 1) \times (N_y - 1)$ points and without boundary conditions for the pressure P .

NUMERICAL SCHEME

To solve the problem defined by equations (1)–(4), a second-order finite-difference discretization in time and a spectral discretization in space are used.

Discretization

The convection and diffusion terms in equation (1) are treated in the same way by an Adams–Bashforth scheme. For inhomogeneous flows, with no-slip boundary conditions, the stability of that scheme is ensured by these boundary conditions.⁹ As explicit schemes require very small time steps for stability, an implicit treatment is introduced. The computation is performed in two steps; the first one is written

$$L_x L_y (\tilde{\mathbf{U}} - \mathbf{U}^n) = \delta t \left[\frac{3}{2} \mathbf{H}^n - \frac{1}{2} \mathbf{H}^{n-1} - \nabla P^n \right], \quad (7)$$

and the second one is

$$L_x L_y (\mathbf{U}^{n+1} - \tilde{\mathbf{U}}) = -\delta t \nabla (P^{n+1} - P^n), \quad (8)$$

where

$$\mathbf{H}^n = -(\mathbf{U}^n \cdot \nabla) \mathbf{U}^n + \nu \Delta \mathbf{U}^n, \quad \text{with } \nu = \frac{2}{Re}, \quad (9)$$

and

$$L_x = 1 - \eta \frac{\partial^2}{\partial x^2}, \quad L_y = 1 - \eta \frac{\partial^2}{\partial y^2},$$

with

$$\eta = O(\nu \delta t, \mathbf{U}^2 \delta t^2). \quad (10)$$

L_x and L_y are implicit operators, that are approximated by centred finite-difference schemes as follows:

$$\frac{\partial^2 f}{\partial x^2} \Big|_{i,j} \# 2 \left[\frac{f_{i-1,j}}{h_i(h_i + h_{i+1})} - \frac{f_{i,j}}{h_i h_{i+1}} + \frac{f_{i+1,j}}{h_{i+1}(h_i + h_{i+1})} \right], \quad (11)$$

where $h_i = x_{i-1} - x_i$. The same kind of relation is used for $\frac{\partial^2 f}{\partial y^2} \Big|_{i,j}$.

$\tilde{\mathbf{U}}$ (equation (7)) is a predictor for the velocity \mathbf{U}^{n+1} . Equation (8) is solved on the classical grid. The coefficient \mathbf{H}^n (equation (9)) is calculated by a collocation method, with the derivatives computed by formal derivation expansions in Chebyshev polynomials of the first kind.¹⁰

The pressure P is determined on the staggered grid and later computed by means of Chebyshev extrapolation on the classical grid.

By extrapolation we shall mean a process to obtain values on the classical grid from those on the staggered grid and by interpolation a process to obtain values on the staggered grid from those on the classical grid.

Velocity–pressure computation

The direct process to compute the pressure is the following: by multiplying equation (8) by

$(L_x L_y)^{-1}$, we obtain

$$\mathbf{U}^{n+1} - \tilde{\mathbf{U}} = -\delta t (L_x L_y)^{-1} \nabla (P^{n+1} - P^n). \quad (12)$$

By taking the divergence of equation (12), and because equation (2) has to be satisfied at time $n + 1$, we obtain

$$\nabla \cdot \tilde{\mathbf{U}} = \delta t \nabla \cdot (L_x L_y)^{-1} \nabla (P^{n+1} - P^n). \quad (13)$$

where $\nabla \cdot (L_x L_y)^{-1} \nabla = A$ is the operator connecting variations of pressure to velocity divergence.

The pressure variation is obtained by solving equation (13) on the staggered grid, namely

$$A(P^{n+1} - P^n) = \frac{1}{\delta t} \nabla \cdot \tilde{\mathbf{U}}. \quad (14)$$

Exact computation of this pressure variation would give a velocity at time $(n + 1)$ satisfying the continuity equation.

The square matrix A has $[(N_x - 1) \times (N_y - 1)]^2$ elements (for example, if $N_x = N_y = 33$, the matrix contains 1,048,576 elements). It is so large that we can only solve equation (14) by an iterative process using a matrix B . This new matrix is built with a small number of A diagonals. B is then modified to become an approximate factorized $\mathcal{L} \cdot \mathcal{U}$ matrix.¹¹ This point is explained in the next section.

So, at each time level, pressure will be obtained as the limit of a sequence of approximations:

$$P_0^{n+1} \dots P_l^{n+1} \rightarrow P^{n+1}.$$

The iterative process stops when the velocity divergence, computed from equation (12), is smaller than a given value ε .

The pressure is determined by a relaxation process. Other methods could be used such as gradient methods.

At iteration l , equation (14) becomes (with $\mathcal{L} \cdot \mathcal{U} \# A$)

$$\mathcal{L} \cdot \mathcal{U} (P_{l+1}^{n+1} - P_l^{n+1}) = \frac{1}{\delta t} \nabla \cdot \tilde{\mathbf{U}} - A (P_l^{n+1} - P^n).$$

And, by means of equation (12), we obtain

$$\mathcal{L} \cdot \mathcal{U} (P_{l+1}^{n+1} - P_l^{n+1}) = \frac{1}{\delta t} \nabla \cdot \mathbf{U}_{l+1}^{n+1}. \quad (15)$$

So the pressure is obtained on the staggered grid by

$$P_{l+1}^{n+1} = P_l^{n+1} + \sigma \left\{ [\mathcal{L} \cdot \mathcal{U}]^{-1} \left[\frac{1}{\delta t} \nabla \cdot \mathbf{U}_{l+1}^{n+1} \right] \right\}, \quad (16)$$

where σ is an under-relaxation coefficient.

The pressure P_{l+1}^{n+1} is then computed on the classical grid by means of a Chebyshev extrapolation.

Finally, \mathbf{U}_{l+1}^{n+1} is computed by solving the system

$$L_x L_y (\mathbf{U}_{l+1}^{n+1} - \tilde{\mathbf{U}}) = -\delta t \nabla (P_l^{n+1} - P^n), \quad (17)$$

taking into account the boundary conditions on the velocity.

Because the operators L_x and L_y are centred finite-difference schemes (equation (11)), equation (17) gives a tridiagonal system, easily solved on the classical grid.

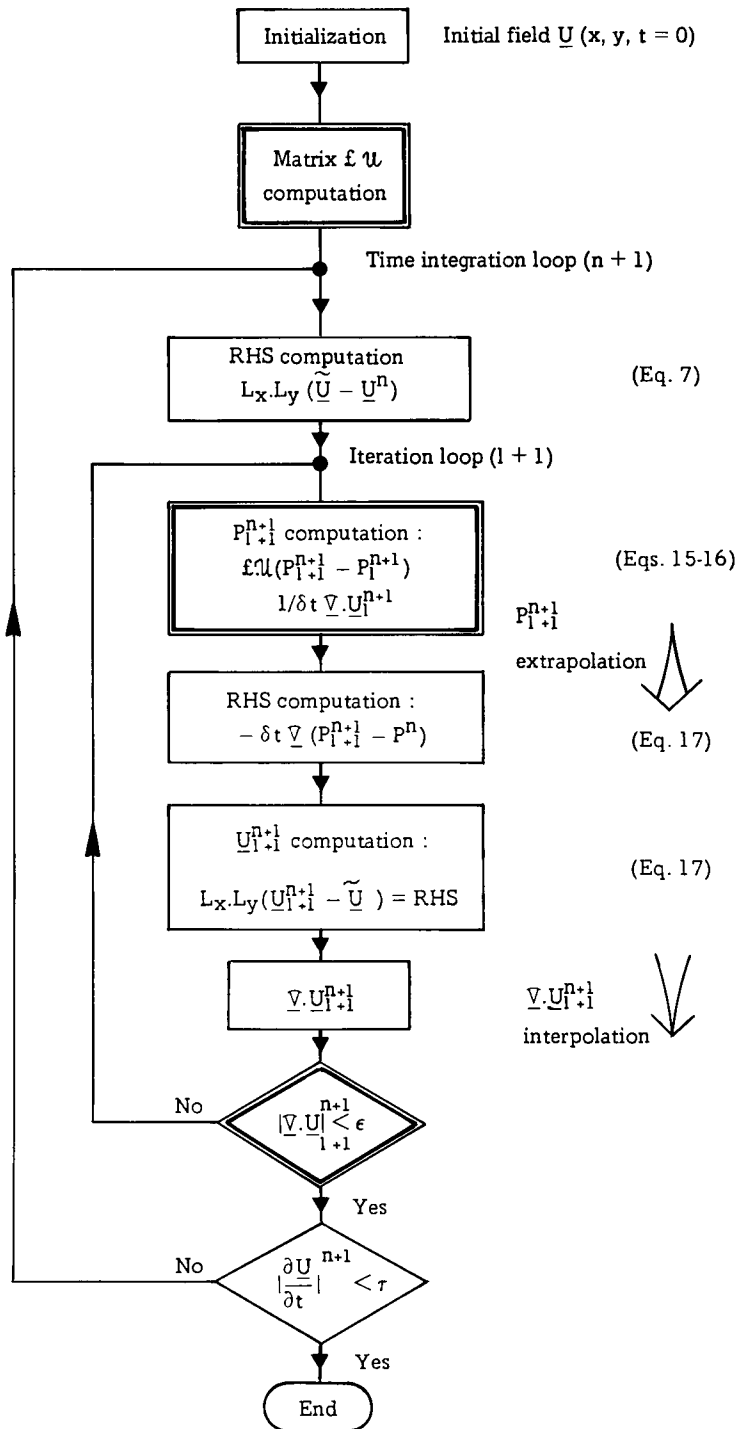


Figure 2. Program organization: computation on classical grid; computation on staggered grid; \Rightarrow extrapolation; \Rightarrow interpolation

Figure 2 gives the program organization. A test is added at the end to see whether the problem (see the section on the 'square cavity' regularized problem) has become stationary.

COMPUTATION OF THE ARTIFICIAL COMPRESSIBILITY MATRIX A

Computation of the matrix A

The matrix A is computed numerically column by column with the following technique: we set

$$Q^i(x_j) = \delta_{ij}, \tag{18}$$

where δ_{ij} is the Kronecker delta symbol; we then compute D^i so that

$$AQ^i = D^i. \tag{19}$$

It contains the $(N_x - 1) \times (N_y - 1)$ elements of the i th column in the matrix A . Figure 3 gives the numerical technique for the calculation of the matrix A .

L_x and L_y are approximated by centred finite-difference schemes with five points (equation (11)); the operator ∇ is approximated by spectral technique by means of Chebyshev polynomials of the first kind.

This very large matrix A with $[(N_x - 1) \times (N_y - 1)]^2$ elements is singular. Only seven parasite modes are removed with the staggered grid. The constant mode is kept.

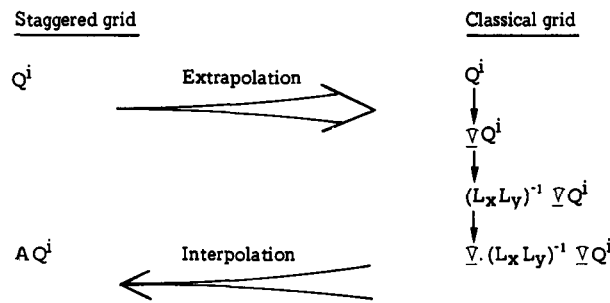
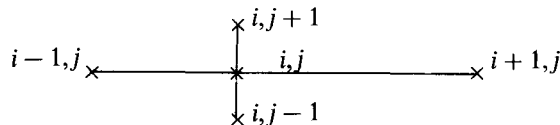


Figure 3. Matrix A computation scheme

Approximation of the matrix A by the matrix B

The matrix B is calculated by analogy with finite-difference schemes. Two possibilities are chosen:

1. Only the principal diagonal of A is kept for building B . In that case, equation (14) is solved directly without $\mathcal{L} \cdot \mathcal{U}$ factorization.
2. The other possibility is to keep five diagonals of A . These diagonals correspond to the five points of the finite-difference scheme:



The matrix B is presented in Figure 4.

Only $5(N_x - 1)(N_y - 1)$ words are used for computer storage of the matrix B .

Approximate $\mathcal{L} \cdot \mathcal{U}$ factorization

To solve equation (15) we use an approximate $\mathcal{L} \cdot \mathcal{U}$ factorization of B . For each triangular

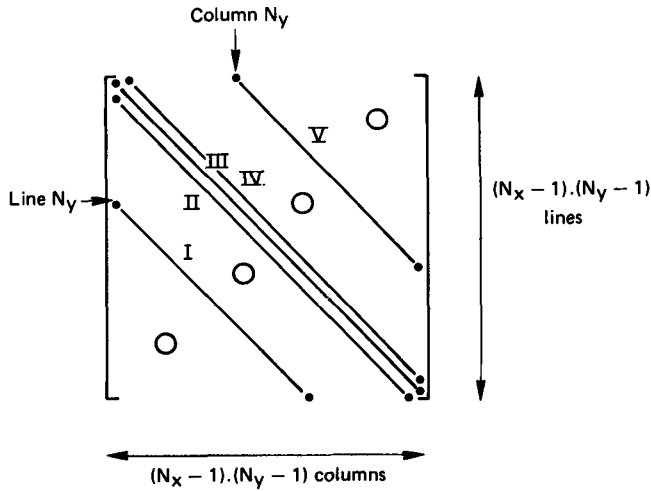


Figure 4. Matrix B with five diagonals

matrix, \mathcal{L} : lower or \mathcal{U} : upper, a tridiagonal form is chosen. Figure 5 shows the decomposition. Each matrix contains three diagonals. All main diagonal elements of \mathcal{L} are 1.¹¹

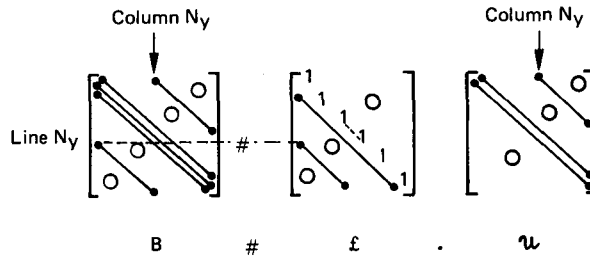


Figure 5. Matrix B : approximate factorized $\mathcal{L}\mathcal{U}$ matrix

Iterative process convergence

To obtain values of the parameters η and σ , we study, numerically, the convergence of the

Table I. Convergence parameters

$Re = 2,$		$N_x = N_y = 9$	
η	10^{-1}	10^{-2}	10^{-3}
σ	0.1	0.1-0.8	0.1
$Re = 200,$		$N_x, N_y = 17$	
η	10^{-1}	10^{-2}	10^{-3}
σ	0.1	0.1-0.6	0.1-0.5

iterative process at the first time step of the computation of the square cavity regularized problem. Two cases are considered: $Re = 2$ and $Re = 200$, with two forms for the $\mathcal{L}\cdot\mathcal{U}$ matrix by analogy with finite-difference schemes: one diagonal and five diagonals.

Table I gives the various values of η and σ for which convergence is obtained with five diagonals for the $\mathcal{L}\cdot\mathcal{U}$ matrix. We have observed that the convergence is quickly reached for a value of the implicit parameter η equal to 10^{-2} . In this case, the under-relaxation parameter σ varies between 0.1 and 0.6 for $Re = 200$.

For a one-diagonal matrix B , the results are not very different. So it seems that the number of diagonals is not a determinant factor of the η parameter.

SQUARE CAVITY REGULARIZED PROBLEM

To test the above algorithm, we compute the stationary solution for a viscous flow in a two-dimensional square cavity with the following regularized boundary conditions:

$$\mathbf{U}_B \begin{cases} U = V = 0 \text{ for } x = 1 \text{ or } x = -1, \forall y \in [-1, +1] \text{ and for } y = -1, \forall x \in [-1, +1], \\ U = -(1 - x^2)^2 \text{ for } y = +1, \forall x \in [-1, +1], \\ V = 0. \end{cases} \quad (20)$$

The initial conditions are chosen such as:

$$\mathbf{U}_0 \begin{cases} U_0 = -(1 - x^2)(1 + y)/2 \\ V_0 = 0, \forall (x, y) \in [-1, +1]^2. \end{cases} \quad (21)$$

This initial field satisfies boundary conditions but not continuity (equation (2)).

The stationary solution is obtained when the time derivative $|\partial\mathbf{U}/\partial t|$ is less than a threshold τ :

$$\max_{i,j} \left| \frac{\partial\mathbf{U}}{\partial t} \right|_{i,j}^{n+1} \# \max_{i,j} \left| \frac{\mathbf{U}^{n+1} - \mathbf{U}^n}{\delta t} \right| \leq \tau. \quad (22)$$

For the iterative process, the convergence threshold is $\varepsilon = 10^{-6}$. The stationary solution is obtained for $\tau = 10^{-6}$. The other parameters are defined in Table II.

One- and five-diagonal cases for A have been studied. The computation for the one diagonal case is 40 per cent more expensive than for the five-diagonal case, because many iterations are necessary

Table II. Computation parameters used for the square cavity regularized problem

N_x N_y	Re	δt	σ	η	Number of diagonals in matrix B .
9	2	10^{-3}	0.9	10^{-2}	1
17	200	10^{-3}	0.7	10^{-2}	
9	2	10^{-2}	0.8	1.5×10^{-2}	5
17	200	10^{-2}	0.6	10^{-2}	

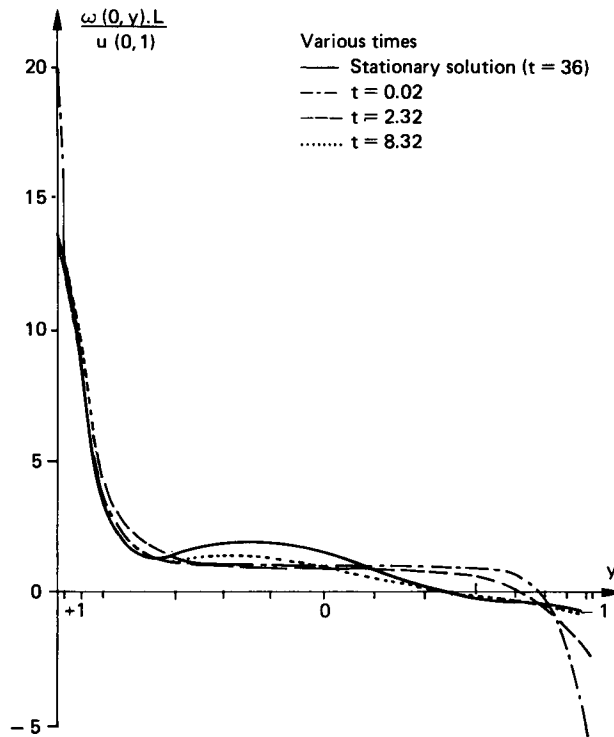


Figure 6. Time history of the vorticity along the axis $x = 0$ in a square cavity at $Re = 200$ and $N_x = N_y = 17$

for the iterative process convergence when the matrix B contains only one diagonal.

Results are given for a five-diagonal matrix computation.

Figure 6 shows the non-dimensional vorticity $\omega(0, y)L/U(0, 1)$ ($L = 2$ is the cavity side length) on the central vertical axis, for various times up to the stationary solution $t = 36$. The Reynolds number is $Re = 200$ and the space discretization is $N_x = N_y = 17$. In Figure 7, isovorticity lines are presented for the same computation case.

A comparison between the pseudo-spectral space-time method and the present method is given in Figure 8.^{3,10} There is a very good agreement between these two methods.

Remark

A Chebyshev extrapolation has been used for drawing the picture of the pseudo-spectral space-time method. It is the main reason of the difference between the two figures (Figure 8).

PRESSURE RESULTS FOR THE SQUARE CAVITY

Figure 9 shows isobar lines with a space discretization of 16×16 points for the stationary solution. No parasite oscillation appears. Yet, a spurious mode exists in the pressure decomposition.¹²

In the method described above, the pressure is expanded in a series of Chebyshev polynomials of the first kind as

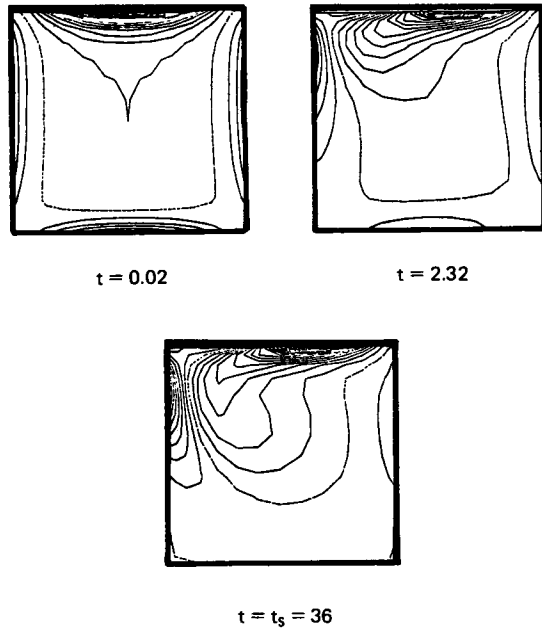


Figure 7. Time history of iso-vorticity lines in a square cavity at $Re = 200$ and $N_x = N_y = 17$

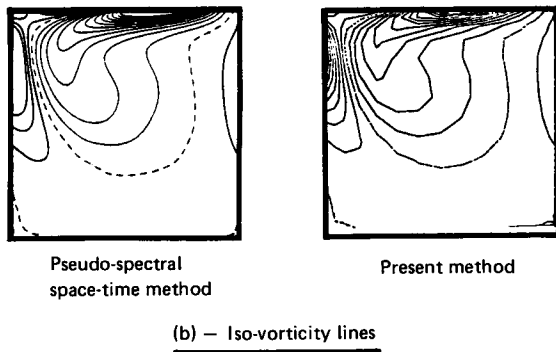
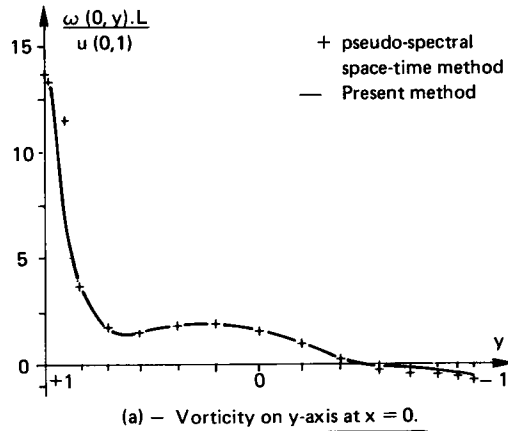


Figure 8. Comparison with the pseudo-spectral space-time method for a square cavity at $Re = 200$ and $N_x = N_y = 17$

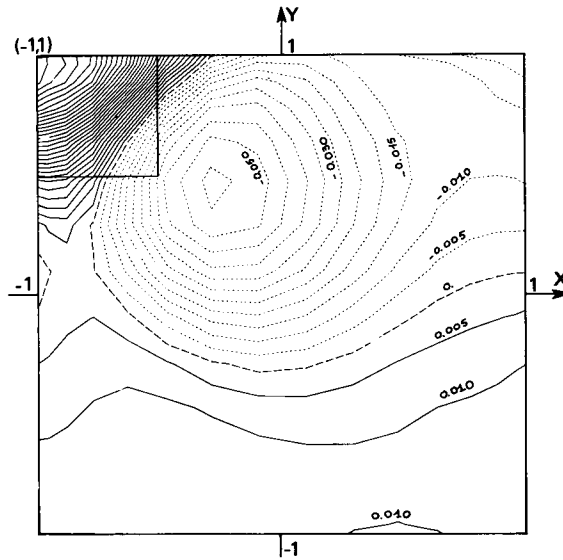


Figure 9(a). Isobar lines in a square cavity at $Re = 200$ and $N_x = N_y = 17$. Stationary solution: $-0.06 \leq \text{pressure} \leq +0.15$ with steps of 0.005; negative pressure; - - - - - zero pressure; ——— positive pressure

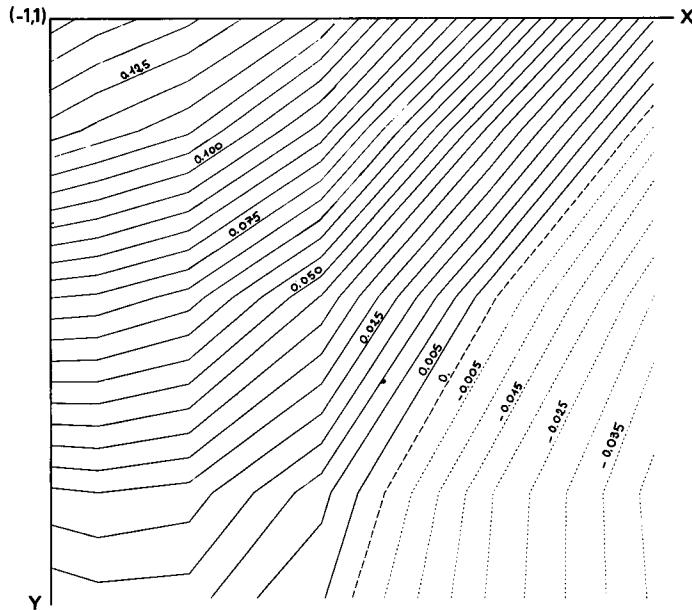


Figure 9(b). Enlargement of the square region at the top left of Figure 9(a). Key as for Figure 9(a)

$$P(x, y) = \sum_{m=0}^M \sum_{n=0}^M a_{m,n} T_m(x) T_n(y). \tag{23}$$

The spurious mode is the (M, M) harmonic of the pressure expansion in series of Chebyshev derivative polynomials $T'_m(x) T'_n(y)$ as

$$P(x, y) = \sum_{m=0}^M \sum_{n=0}^M b_{m,n} T'_m(x) T'_n(y). \quad (24)$$

Classical properties of Chebyshev polynomials give the relation

$$b_{M,M} = \frac{1}{4M^2} a_{M-1,M-1}. \quad (25)$$

For example, the numerical values of $b_{M,M}$ are the following:

$$b_{8,8} = 10^{-5}, \quad b_{16,16} = 4 \times 10^{-8}.$$

As soon as the discretization M is high ($M > 16$), the value of the spurious mode is too small to induce parasite oscillations.

Arbitrarily, we have modified the $a_{M-1,M-1}$ harmonic at $t = 0.01$ (\blacktriangledown in Figure 10) and at $t = 45$ (\blacklozenge in Figure 10). The pollution appears as a constant on odd harmonics $a_{2l+1,2l+1}$ only. Figure 11 shows isobar lines of the stationary solution with a modification of the $a_{M-1,M-1}$ harmonic at $t = 0.01$.

The pressure gradient and the velocity are not modified even if the pressure expansion presents a checkerboard harmonic.

CONCLUSION

The above iterative algorithm for computing the pressure gives very accurate results.

This way of determining pressure by solving the continuity equation is consistent with the Navier–Stokes problem in which boundary and initial conditions are only given for the velocity. In our present case, no boundary conditions are necessary for the pressure.

To improve the efficiency of the method, we could use a more elaborated algorithm for iterative calculation of pressure: ‘steepest descent’, the ‘Axelsson algorithm’, etc.

Computation on a staggered grid for the velocity divergence avoids most of the effects of parasite modes that appear in the classical velocity–pressure formulation and gives us results with a spectral accuracy.

NOTATIONS

A	artificial compressibility matrix
B	approximate matrix of A
L	square cavity side length ($L = 2$)
L_x, L_y	implicit operators: $L_x = 1 - \eta \partial^2 / \partial x^2$, $L_y = 1 - \eta \partial^2 / \partial y^2$
$\mathcal{L} \cdot \mathcal{U}$	approximate factorized matrix of B
N_x, N_y	number of discretization points on x and y axes, respectively
P	pressure
Re	Reynolds number: $Re = U(0, 1)L/v = 2/v$
\mathbf{U}	velocity vector with two components (U, V)
\mathbf{x}	position vector with two components (x, y)
δt	time-step length
Δ	Laplacian operator: $\Delta = \partial^2 / \partial x^2 + \partial^2 / \partial y^2$
ε	convergence threshold for the iterative process
η	implicit operators parameters
ν	kinematic viscosity
σ	relaxation coefficient
τ	convergence threshold for the stationary solution

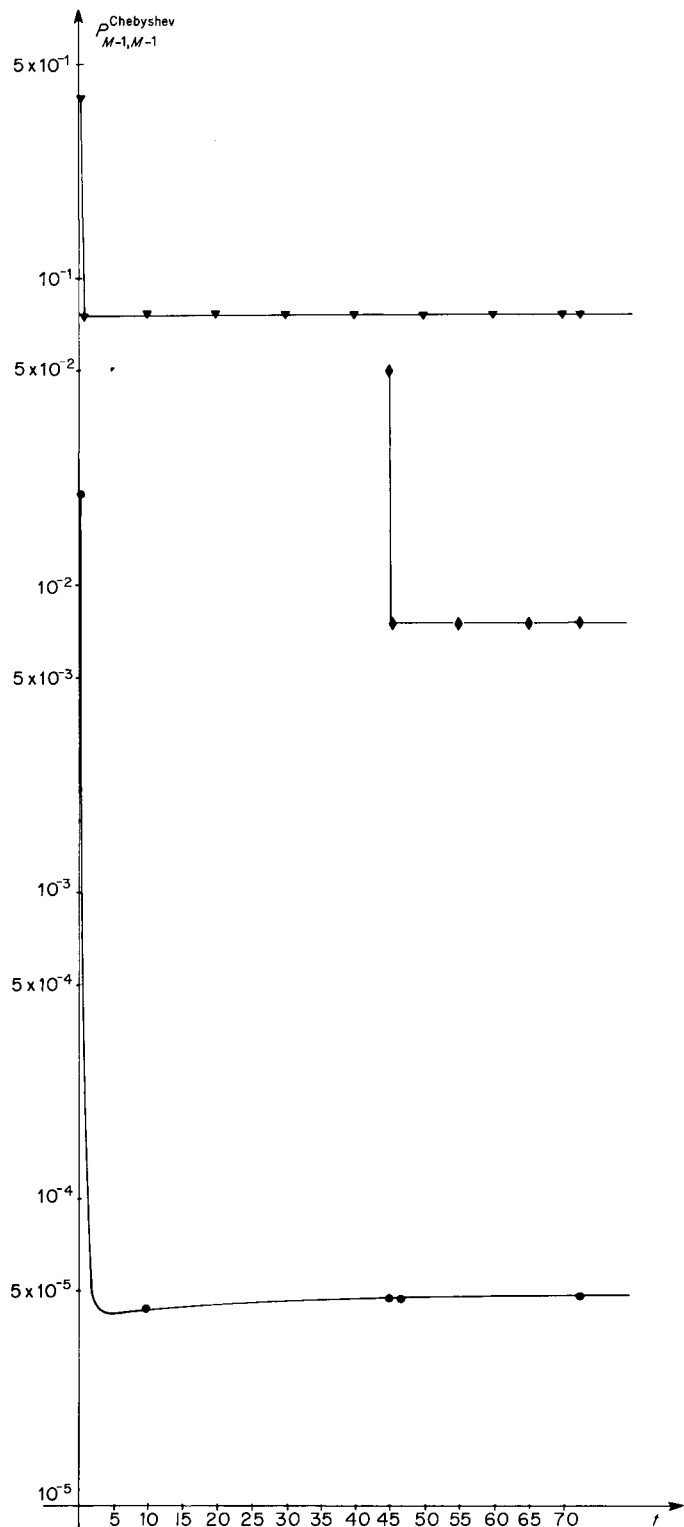


Figure 10. Amplitude of the pressure Chebyshev mode $(M-1, M-1)$ for $M=16$: \bullet — \bullet — no amplification; \blacklozenge — \blacklozenge — amplification at $t=45$; \blacktriangledown — \blacktriangledown — amplification at $t=0.01$

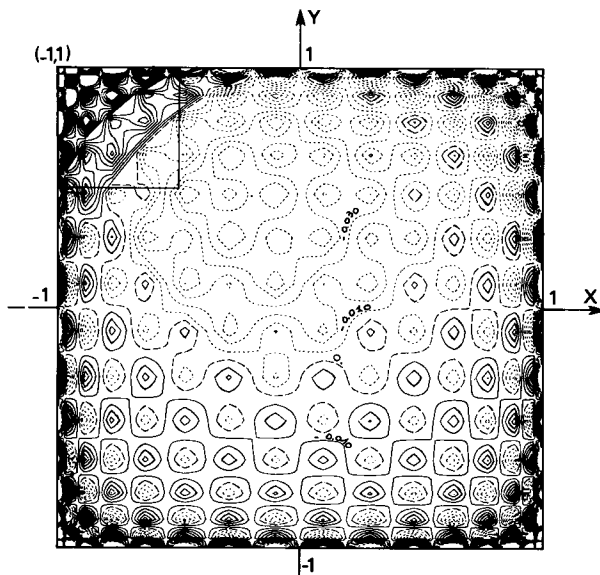


Figure 11(a). Isobar lines in a square cavity at $Re = 200$ and $N_x = N_y = 17$. Stationary solution after amplification at $t = 0.01$: $-0.06 \leq \text{pressure} \leq +0.15$ with steps of 0.005 ; ----- negative pressure; - . - . - zero pressure; ——— positive pressure

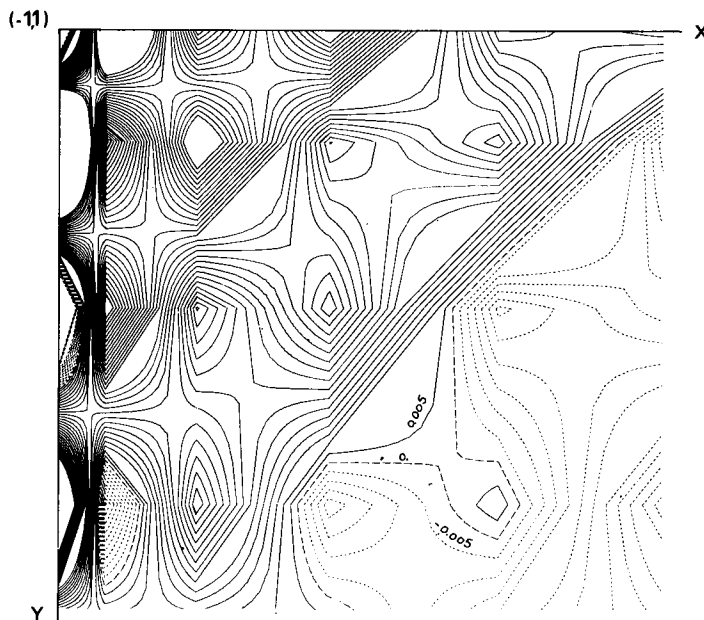


Figure 11(b). Enlargement of the square region, at the top left of Figure 11(a). Key as for Figure 11(a)

REFERENCES

1. M. Deville, L. Kleiser and F. Montigny-Rannou, 'Pressure and time treatment for Chebyshev spectral solution of a Stokes problems.' *Int. j. numer. methods fluids*, **4**, 1149-1163 (1984).

2. R. L. Sani, P. M. Gresho, R. L. Lee and D. F. Griffiths, 'The cause and cure (?) of the spurious pressures generated by certain FEM solutions of the incompressible Navier–Stokes equations: part I', *Int. j. numer. methods fluids*, **1**, 17–43 (1981).
3. F. Montigny-Rannou, 'Influence of compatibility conditions in numerical simulation of inhomogeneous incompressible flows', *Proceedings of the fifth GAMM Conference on Numerical Methods in Fluid Mechanics*, Rome, October 1983; in M. Pandolfi and R. Piva (eds), *Notes on Numerical Fluid Mechanics*, Vol. 7, Vieweg, 1984.
4. M. R. Malik, T. A. Zang and M. Y. Hussaini, 'A spectral collocation method for the Navier–Stokes equations', *Journal of Computational Physics*, **61** (1), 64–88 (1985).
5. Y. Morchoisne, 'Résolution des équations de Navier–Stokes par une méthode de sous-domaines spectraux', *3ème Conférence Internationale sur les Méthodes Numériques de l'Ingénieur GAMNI*, Paris 14–16 March 1983.
6. Y. Morchoisne, 'Inhomogeneous flow calculations by spectral methods: mono-domain and multi-domain techniques', in R. G. Voigt, D. Gottlieb and Y. Hussaini (eds), *Spectral Methods for Partial Differential Equations*, SIAM, Philadelphia, 1984.
7. L. Kleiser and U. Schumann, 'Treatment of incompressibility and boundary conditions in 3-D numerical spectral simulations of plane channel flows', *Proceedings of the Third-Gamm Conference on Numerical Methods in Fluids Mechanics*; in E. H. Hirschel (ed.), *Notes on Numerical Fluid Mechanics*, Vol. 2, Vieweg, 1980.
8. C. Bernardi, Y. Maday and B. Métivet, 'Une méthode directe de collocation pour le problème de Stokes', *Comptes-Rendus Académie des Sciences*, Paris, t302, série I, no. 4, 163–166, 1986.
9. Y. Maday, B. Pernaud-Thomas and H. Vandeven, 'Une réhabilitation des méthodes spectrales de type Laguerre', *La Recherche Aérospatiale*, **1985-6**, 353–275 (1985).
10. Y. Morchoisne, 'Résolution des équations de Navier–Stokes par une méthode pseudo-spectrale en espace-temps', *La Recherche Aérospatiale*, **1979-5**, 293–306 (1979). English Translation—ESA TT-613.
11. D. S. Kershaw, 'The incomplete Cholesky–conjugate gradient method for the iterative solution of systems of linear equations', *Journal of Computational Physics*, **26**, 43–65 (1978).
12. C. Bernardi and Y. Maday, 'A staggered grid spectral method for the Stokes problem', *6ième Colloque International sur la simulation d'écoulements par éléments-finis*, INRIA-Antibes, 16–20 June 1986.